SCA2003-37: EVALUATION OF RECOVERY EFFICIENCY AND RESIDUAL OIL SATURATION OF TWO DISTINCT ARABIAN CARBONATE RESERVOIRS

Taha M. Okasha, James J. Funk and Abdul-Jalil Al-Shiwaish
Saudi Aramco Research and Development Center,
Dhahran, Saudi Arabia

This paper was prepared for presentation at the International Symposium of the Society of Core Analysts held in Pau, France, 21-24 September 2003

ABSTRACT

Saudi Arabia has a variety of carbonate reservoirs of different geologic ages. Such reservoirs are characterized by extremely heterogeneous rock properties. These heterogeneities are caused by the wide spectrum of environments in which carbonates are deposited and subsequent alteration of the original rock fabric.

In this paper, extensive SCAL work was carried out on preserved core plugs recovered from two distinct carbonate reservoirs. The first reservoir is a Late Jurassic Arab-D offshore carbonate reservoir (Abu Safah field). The second one is Shu'aiba reservoir (Shaybah field) located in the Rub' Al-Khali in southeastern Saudi Arabia. The purpose of this study is to provide and evaluate waterflood recovery efficiency and residual oil saturations of the two distinct Arabian reservoirs.

The variation of oil recovery and residual oil saturation between the two distinct reservoirs is due to variations of rock characteristics especially the relationship of textural and diagenetic features which affect the size and distribution of pore throats. Shu'aiba reservoir rock could be classified as wackstone which demonstrates a higher ratio of lime mud to detrital grains (pore sizes ~ 0.27 to 1.5 microns). On the other hand, Arab-D reservoir is classified as grainstone and consists of oolitic limestone and dolomitic limestone with larger pore sizes (0.5 to 5.5 microns).

The test results indicated that pore structure, pore size distribution, rock fabric, and environment of deposition are important factors that affect microscopic oil and water flow in porous media and the development efficiency of an oil field developed by water injection. Oil recovery from Arab-D reservoir (Late Jurassic) is slightly higher than that of Shu'aiba reservoir (Lower Cretaceous). The residual oil saturations values for Arab-D reservoir were also found to be slightly higher than those of Shu'aiba reservoir. The Arab-D reservoir showed less permeability dependence for both (S_{wir} and S_{or}) end point saturations.

INTRODUCTION

Carbonate reservoirs make up about 20 % of the world's sedimentary rocks and contain 40 % of the world's oil. In Saudi Arabia, the current hydrocarbon production is from carbonate reservoirs of Cretaceous and Jurassic age. Such reservoirs are characterized by extremely heterogeneous rock properties. These heterogeneities are caused by the wide spectrum of environments in which carbonates are deposited and subsequent alteration of the original rock fabric.

The Research and Development Center at Saudi Aramco has conducted extensive SCAL work to investigate the displacement characteristics of two distinct Arabian carbonate reservoirs. The first reservoir is Late Jurassic Arab-D offshore carbonate reservoir (Abu Safah field). This field is located approximately 30 miles off the coast of Arabian Gulf. It was discovered in 1963 and has been producing since January 1, 1966. The Arab-D reservoir produces Arabian Medium crude with an average gravity of 30^{o} API and 2.7% sulfur by weight. The second reservoir is Lower Cretaceous Shu'aiba reservoir (Shaybah field), located in the Rub' Al-Khali in southeastern Saudi Arabia. The produced crude has an ^{o}API stock gravity of 41 with low sulfur content. Production from this diagenetic Shu'aiba reservoir began in July, 1998.

Environment of deposition, Diagenetic alteration, and geologic complexity lead to variation of carbonate rock properties and rock type. Late Jurassic Arab-D carbonates are grainstones/packstones formation which was deposited in current-swept shelf environments.[1] Diagenesis is minimal in the Arab-D reservoir, and most of the original porosity is retained.[2] On the other hand, Shu'aiba reservoir consists of non-dolomitic carbonates (mudstones, wackstones, and packstones).[3] It was deposited over an extensive stable platform.[4]

The displacement efficiency, relative permeability curves, and residual oil saturation (S_{or}) can be related to rock characteristics, especially, the relationship of textural and diagenetic features, which affect the size and distribution of pore throat features. A review of studies which relate the variation of oil recovery and residual oil saturation to pore geometry and lithologic character of the reservoir samples showed that a good number of publications on sandstone reservoirs are available.[5-8] Due to the complex heterogeneity of carbonate reservoirs; few publications discussed the effect of pore size, texture, and rock fabric on waterflood displacement efficiency and residual oil saturation. Most of oil/water relative permeability studies on carbonate reservoir samples were conducted at room condition and synthetic fluids were used. Abrams (1975)[9] reported that ROS decreased with increase of capillary number (Nc). Kamath, J.et.al.[10] suggested increase in oil recovery through increase of pressure gradient and decrease in interfacial tension.

In this study, extensive laboratory work was conducted on preserved core plugs to evaluate waterflood recovery efficiency and residual oil saturation of the two distinct Arabian reservoirs (Arab-D reservoir in Abu Safah field and Shu'aiba reservoir in Shaybah field).

Unsteady state relative permeability measurements were performed on lithofacies in both reservoirs using composite core arrangements.[11]

PLUG SELECTION AND TEST FLUIDS

Cores 4 in. in diameter from both reservoirs were obtained using similar processes differing only the material for the inner barrel (fiberglass for Arab-D and aluminum for Shu'aiba). Cores were cut with a bland KCl water base mud. The inner core barrels were cut into three foot sections that were placed into fiberglass or PVC tubes containing nitrogen aerated KCl brine with a minimum of 10,000 ppm TDS.

Core plugs 1.5 inches in diameter were drilled from the whole core at 0.5-foot intervals with preserving brine. The drilling direction was perpendicular to the axis of the whole core. After trimming, the plugs were wrapped with aluminum foil and then placed in sealed container completely submerged in evacuated preserving brine (10,000ppm KCl).

Visual, brine permeability at remaining oil saturation, and CT scans were performed as screening tests to assist in sample selection. The screening tests were combined with a review of conventional core data and geological description of the core material to ensure that anomalous samples were not tested. Cores that were fractured, broken, or displayed brine permeability less than 1 millidarcy (mD) were excluded from further testing.

Recombined live oil samples and methane-saturated brine samples representing the actual oleic and aqueous phases for the two reservoirs were used in relative permeability tests conducted at reservoir conditions. Table 1 presents the composition of the synthetic formation brines, viscosities of fluids, and reservoir conditions for each reservoir.

EXPERIMENTAL PROCEDURE

Relative Permeability Measurements

The unsteady-state relative permeability tests were conducted at simulated reservoir conditions using recombined live oil and synthetic brine similar to reservoir brine.

The procedure for relative permeability measurements included the use of composite core[11] assembled from core material cut with KCl water based mud and preserved at the well site. Cores were flushed with simulated formation brine to remove mud filtrate. Brine permeabilities at the native state remaining oil saturation were determined and used as one of the determining factors for sample selection. Since single reservoir core plugs are relatively short in length (4-8 cm), employing these cores to obtain relative permeabilities can result in relatively high material balance errors. To overcome this shortcoming, several short cores (~4) were stacked together to form a composite core for relative permeability tests. Longer composites reduce saturation uncertainties and in the absence of competing capillary end effects between plugs allows for lower flooding rates. This resulting composite core was then used as a single core with average properties.

In preparation for testing, a brine-saturated composite core was assembled, placed into a rubber sleeve, and loaded into horizontal core holder. Dead oil was flushed through the composite under backpressure to displace gas, ensure complete fluid saturation and to establish an initial Sw. Reservoir conditions were established (Table 1). Recombined live oil was injected to displace the dead oil. After aging for approximately two weeks, the core was stabilized by pumping several pore volumes of live oil at a constant flow rate of $2cm^3$/min, until a constant pressure drop was obtained establishing S_{wi}. At pressure stabilization, baseline oil permeability at S_{wi} was determined. Methane-saturated brine was injected to simulate a waterflood processes. A constant flow rate of 2 cm^3/min was maintained. This rate was chosen to minimize capillary end effects. These effects are minimal when the scaling factor ($L\mu V$) is greater than 2 based on scaling criteria proposed by Rapoport and Leas.[12] L is the core length (cm), μ is displacing phase viscosity (centipoises) and V = q/A is flow rate per unit cross-sectional area of the composite core (cm/min). Both oil and water volumes were measured at reservoir condition by an acoustically monitored separator. Relative permeabilities were calculated using JBN method.[13]

At the end of waterflooding, the core composite was allowed to cool. All extruded fluids were collected. The core holder was disassembled. The cores were weighed and placed in the Dean Stark extraction apparatus where water and oil were extracted using toluene. The core plugs were then placed in a vacuum oven where they were dried at 150 ^oF for two days. Air permeability and porosity for each plug was measured at net confining stress.

Mercury Injection Measurements

Mercury injection capillary pressure and pore sizes were measured using a Ruska mercury injection system. The test consists of two runs; blank run (without sample) and a sample run. The readings of blank run represent the compression effects and mercury intrusions into small spaces in the interior part of the apparatus as a result of incremental increase of applied pressure. Each run includes an injection test in a vacuumed system followed by an ejection test.[14]

The difference between the blank run and the sample run represent the volume of mercury introduced in the pores during the injection test and the volume of mercury expelled from the pores during the ejection test.

RESULTS

Oil Recovery and Relative Permeability

Reservoir engineering studies rely heavily on measurements from a few samples from reservoir rock formations. Core plugs relative permeability is a key measurement, because it gives one of the few insights into multiphase flow behavior. The estimation of reserves and recoverable hydrocarbons for a whole field may depend quite strongly on the values

determined for endpoint saturations and relative permeability curves from some limited core dataset.

Seven composite cores from the dominant facies of each reservoir (Shu'aiba and Arab-D) were tested with water flood experiments. These composites were selected based on variations of reservoir rock properties and facies. They provide more precise data because the pore volume and pressure drop are both larger, and are less impacted by capillary and inlet end effects. Tables 2 and 3 summarize the recovery performance and rock properties of the seven composite cores that were used in the relative permeability experiments from Shu'aiba and Arab-D reservoir, respectively.

As illustrated by other authors[8,10], several parameters can affect the overall recovery. These include displacement rate, displacement pressure, wettability heterogeneity and structural heterogeneity. Using a consistent experimental protocol for both reservoirs, variations of these parameters were minimized. Although there are differences in interfacial tensions for the two oil/brine systems (Arab-D 36 dynes/cm, Shu'aiba 32 dynes/cm) and viscosities (Table 1) the dominate difference and the basis for our comparison is in the pore structure.

Results in Tables 2 and 3 showed an oil recovery variation of 25.6 % of pore volume (50.7% to 76.3%) for Shu'aiba composites and 10.9 % of pore volume (60.1 to 71 %) for Arab-D composites. The residual oil saturation (S_{or}) had a variation of 24.8% of pore volume for Shu'aiba composites and 8.9% for Arab-D composites. The irreducible water saturation (S_{wir}) variation was 24.8 % or pore volume for Shu'aiba composites and 17.3 % of pore volume for Arab-D composites. The average oil recovery from Arab-D reservoir is slightly higher (65.6 % of pore volume) than that of Shu'aiba reservoir (63.3 % of pore volume). The average residual oil saturations value for Arab-D reservoir was found to be higher (22.3 %) than that of Shu'aiba reservoir (18.2 %). The permeability to oil at irreducible water saturation ranged from 0.5 to 10.4 mD for Shu'aiba composites; while it varied between 1.3 to 423 mD for Arab-D composites. Variations in oil recoveries, S_{wir}, and S_{or} between the two distinct reservoirs are related to complex diagenetic and environment of deposition effects which result in differences in rock permeability, pore size, and pore size distribution.

Figures 1 and 2 show semi-log plots of relative permeability curves versus water saturation ratio for the tested composites from Shu'aiba and Arab-D reservoirs, respectively. Figure 1 indicates that four Shu'aiba water relative permeability curves (Krw) coincide (composites #1, 2, 4, and 5). Figure 2 shows that four Arab-D Krw curves coincide (composites# 1, 4, 6, and 7) with the remaining three coinciding at higher water saturations. As can be observed from these figures, oil relative permeability curves (Kro) fall into wider bands than Krw curves and in the Shu'aiba samples cover a broader range of residual saturations.

Figures 3 and 4 show plots of irreducible water saturation *vs* stressed permeability for the composites tested from Shu'aiba and Arab-D reservoirs. Both figures reflect a trend of increasing S_{wir} with increasing permeability. The trend is more pronounced for the Shu'aiba

samples. Figures 5 and 6 show plots of residual oil saturation *vs* stressed permeability for the composites tested from Shu'aiba and Arab-D reservoirs, respectively. As shown in these figures, there are two types of trends: residual oil saturation decreasing with increasing permeability for Shu'aiba composites (Figure 5) and residual oil saturation increasing with permeability for Arab-D composites (Figure 6).

Mercury Injection

The distribution of immiscible fluids within the pores of porous media depends on the capillary pressure. Capillary pressure data obtained by mercury injection method can be transformed to evaluate the pore size distribution of the reservoir rock. The size and distribution of pore throats within reservoir rock controls its capillary pressure characteristics, which in turn control fluid behavior in the pore system.

Mercury injection capillary pressure results show that Shu'aiba carbonate materials display primarily uni-modal with some bimodal distributed pore systems as indicated in Figure 7. Such distributions reflect the diagenetic history. Figure 8 shows the more complex bimodal and tri-modal distribution of pore systems in the Arab-D samples. Figures 9 and 10 present plots of cumulative wetting phase saturation *vs* the pore entry radius of plugs from Shu'aiba and Arab-D reservoirs, respectively. They indicate that the median pore radius of Shu'aiba samples ranged from 0.27 to 1.5 microns, while those for Arab-D samples vary between 0.5 to 5.5 microns.

DISCUSSION

The variation of oil recovery, residual oil saturation, and the oil/water relative permeability curves between Shu'aiba (Shaybah field) and Arab-D reservoirs (Abu-Safah field) could be related to the difference between the two reservoirs in terms of rock fabric, pore size distribution and permeability.

Core description of the tested and adjacent plugs, petrographic examination, and thin section analyses were investigated for both reservoirs material. Overall, the Arab-D reservoir material could be classified as grainstone which consists of oolitic and dolomitic limestone. The reservoir is a composite cyclic arrangement of grain-dominated and mud-dominated carbonates. Thin sections reveal a framework of skeletal grains that supports a system of pores dominated by inter-particle and intra-particle porosity. Grainstones, made up mainly of rounded equant to elongated pelletoids and locally occurring grains that resemble ooids is the most abundant texture (Figures 14-16). This fabric revealed an average reservoir porosity of 24.4 % of pore volume and permeability of 440 mD. Also, this reflects large range of pore radius from 0.5 to 5.5 μm.

On the other hand, petrographic examination and thin section analyses of Shu'aiba reservoir rock showed that the reservoir consists of non-dolomitic soft carbonates (wackstones and packstones). The formation is heterogeneous and indicates a lower ration

of lime mud to detrital grains. Dominant porosity is primary micro-porosity developed in the inter-granular mud matrix. Secondary was developed through the dissolution of biogenic fragments and mud matrix (Figures 11 -13). Hence, complex diagenetic alteration of original rock fabric and high ratio of lime mud to detrital grains reduces the permeability (13 mD) of Shu'aiba reservoir. Consequently, the pore radius becomes smaller and ranges from 0.27 to 1.5 microns.

Comparison of results in Tables 2 and 3 showed that average S_{wir} (12.13 %) for Arab-D reservoir is lower than average S_{wir} (18.44 %) of Shu'aiba reservoir. This is because Arab-D reservoir rock has larger pores and consequently smaller surface area. Shu'aiba reservoir rock with smaller pore sizes has a higher average S_{wir} due to a larger surface area which leaves little room for the flow of mobile fluids. The lower permeability rocks exhibit lower S_{wir}. This behavior was observed also by Morgan and Gordon, 1970[15]. The recovery efficiency of tight Shu'aiba reservoir was less than that of Arab-D reservoir due to diagentic alteration of rock fabric, texture and smaller pore sizes of Shu'aiba rock.

The behavior of S_{wir} and S_{or} and consequently oil recovery is related in characteristic ways to the effect of rock fabric and diagenesis. These relations are not captured in standard correlations and expectations based strictly on permeability. A strong diagenetic over print such as that seen in the Shu'aiba samples does provide expected saturation variations and recovery. However, minimum diagenesis and less change in rock fabric of the Arab-D samples revealed larger permeability variation but less variation in saturation and recovery.

CONCLUSIONS

1. Variation in rock fabric, diagenetic alteration, and pore size distribution affect Unsteady-state oil/water relative permeability results and recovery efficiency of two Saudi carbonate reservoirs with different geologic ages.
2. Water flood results showed that oil recovery from Arab-D reservoir (Late Jurassic, Abu Safah field) is higher than that of Shu'aiba reservoir (Lower Cretaceous, Shaybah field). The average residual oil saturations for Arab-D reservoir samples were found to be higher than those of Shu'aiba reservoir samples although only at a confidence interval of 75% primarily due to the large standard deviation of the Shu'aiba results. The irreducible water saturation values for Arab-D reservoir were much lower than those of Shu'aiba reservoir.
3. Residual oil saturation tends to decrease with permeability for Arab-D reservoir (high permeability rock) while tight rock with low permeability (Shu'aiba reservoir) tends to show an opposite trend. The high residual oil saturations in the two lowest permeability Shu'aiba samples support the idea that in samples with similar structural characteristics, other factors such as displacement pressure may be significant.
4. Shu'aiba reservoir rock could be classified as wackstone (uni-modal and bimodal systems) which demonstrates a lower ratio of lime mud to detrital grains (pore sizes ~ 0.27 to 1.5 microns). On the other hand, Arab-D reservoir is classified as grainstone and

consists of oolitic limestone and dolomitic limestone (bimodal and tri-modal systems) with larger pore sizes (0.5 to 5.5 microns).

ACKNOWLEDGEMENTS

Appreciation is given to the Saudi Arabian Oil Company (Saudi Aramco) for granting permission to present and publish this paper. The authors wish to thank the management of Research and Development Center. Special thanks to Petrophysics Unit personnel for their efforts in experimental work.

REFERENCES

1. Ayres, M.G., Bilal, M., Jones, R.W., Slentz, L.W., Tartir, M., and Wilson, A.W.: "Hydrocarbon Habitat in Main Producing Areas, Saudi Arabia," The American Association of Petroleum Geologist Bulletin, Vol. 66, No. 1, January 1982, p.1-9.
2. Powers, R.W.: "Arabie Saoudite. Lexique Stratigraphique International" V.III Asie, fasc.10b. Centre National de la Recherche Scientifique, Paris, 177p.
3. Dunham, R.J.: "Classification of Carbonate Rocks According to Depositional Texture" AAPG Memoir, Norman, OK, 1961.
4. Hughes, G.W.: "Bioecostratigrahy of the Shu'aiba Formation, Shaybah Field, Saudi Arabia" GeoArabia, Vol. 5, No. 4, P. 545-578.
5. Morgan, T.J., and Gordon, D.T.: "Influence of Pore Geometry on Water-Oil relative Permeability," JPT, October, 1970, p. 1199-1208.
6. Kevin Li, Yirong, J., Zhijian, D., and Ying, H.: "The Oil-Water Relative Permeability of A Low Permeable Reservoir," paper SPE 30001 presented at the International Meeting on Petroleum Engineering held in Beijing, PR China, 14-17 November 1995.
7. Behrenbruch, P.: "Waterflood Residual Oil Saturation-The Buffalo Field, Timor Sea," paper SPE 64282 Presented at the SPE Asia Pacific Oil and Gas Conference and Exhibition held in Brisbane, Australia, 16-18 October 2000.
8. Skauge A., and Ottesen B.: "A Summary of Experimentally Derived Relative Permeability and Residual Saturation on North Sea Reservoir Cores," paper SCA2002-12, presented at 2002 International Symposium of the Society of Core Analysts held in Monterey, California, 22-25 September, 2002.
9. Abrams, A.: "The Influence of Fluid Viscosity, Interfacial Tension, and Flow Velocity on Residual Oil Saturation left by Waterflood," SPEJ (October 1975), p.437-447.
10. Kamath, J.,Meyer, R.F., Raytheon, M., and Nakagawa, F.M.: "Understanding Waterflood Residual Oil Saturation of Four Carbonate Rock Types," paper SPE 71505, presented at the 2001 SPE Annual Technical Conference and Exhibition held in New Orleans, Louisiana, 30 September-3 October 2001.
11. Huppler, J.D.: "Waterflood Relative Permeabilities in Composite Cores," J. Pet.Tech, May 1969, 539-540.
12. Rapoport, L.A., and Leas, W.J.: "Properties of Linear Water Floods," Trans., AIME (1953), 198, 139-148.
13. Johnson, E.F., Bossler, D.P., and Nauman, V.O.: "Calculation of Relative Permeability from Displacement Experiments," Trans., AIME (1959) 216, 370.
14. Brown, H. W.: "Capillary Pressure Investigation," Petroleum Transactions, AIME, Vol. 192, (1951), 67.
15. Morgan, T. J., and Gordon D. T.: "Influence of Pore Geometry on Water-Oil Relative Permeability" J. Pet.Tech, October 1975, 1199-1208.

TABLE 1- Brine Composition and Reservoir Conditions for Both Reservoirs.

	Arab-D Reservoir	**Shu'aiba Reservoir**
Variable		**Value**
Sodium Chloride, g/L	16.70	66.35
Calcium Chloride, g/L	3.62	20.85
Magnesium Chloride, g/L	1.28	7.07
Sodium Bicarbonate, g/L	--	0.52
Sodium Sulfate, g/L	--	0.60
Brine Viscosity, cP	0.39	0.42
Oil Viscosity, cP	2.5	0.48
Reservoir Temperature, ^{o}F	192	195
Net Confining Pressure, psig	3,250	2,500

TABLE 2 – Summary of Waterflood Performance properties Data for Composite Cores (Shu'aiba Reservoir, Shaybah Field).

Composite No.	**Average Permeability to Air (mD)**	**Average Porosity (%)**	**Final Oil Recovery (% PV)**	**S_{wir} (% PV)**	**S_{or} (% PV)**	**Ko at S_{wir} (mD)**
1	5.6	24.0	50.7	18.6	30.7	2.47
2	9.5	27.4	76.3	17.1	6.5	3.48
3	6.4	26.7	69.8	14.6	15.6	2.6
4	6.0	26.1	74.0	6.9	19.1	1.9
5	13.0	20.1	57.3	32.2	10.5	10.4
6	15.3	28.2	52.2	34.0	13.6	7.1
7	1.9	15.9	63.0	5.6	31.3	0.5

TABLE 3 – Summary of Waterflood Performance properties Data for Composite Cores (Arab-D Reservoir, Abu Safah Field).

Composite No.	**Average Permeability to Air (mD)**	**Average Porosity (%)**	**Final Oil Recovery (% PV)**	**S_{wir} (% PV)**	**S_{or} (% PV)**	**Ko at S_{wir} (mD)**
1	423.0	23.6	60.1	14.9	24.9	264
2	13.5	27.2	71.0	11.4	17.5	11.0
3	34.3	27.5	61.4	12.3	26.2	1.3
4	94.6	26.9	62.4	20.3	17.3	72
5	80.0	25.4	63.4	12.8	23.8	74
6	96.2	24.8	70.5	3.3	26.2	35
7	106.5	23.4	70.1	9.9	20.0	42.0

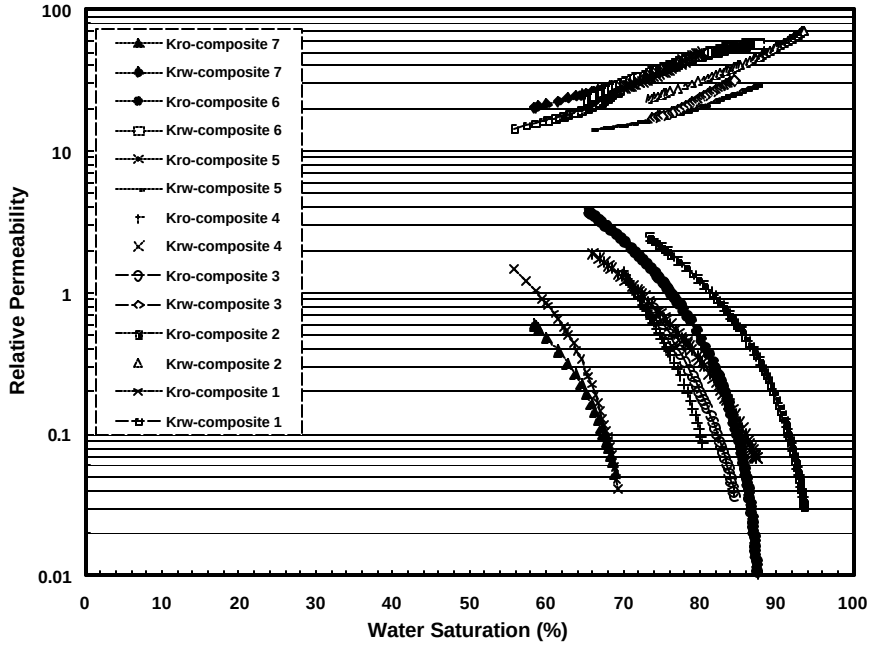

Figure 1: Unsteady-State Oil/Water Relative Permeability Curves for Shu'aiba Reservoir, Shaybah Field.

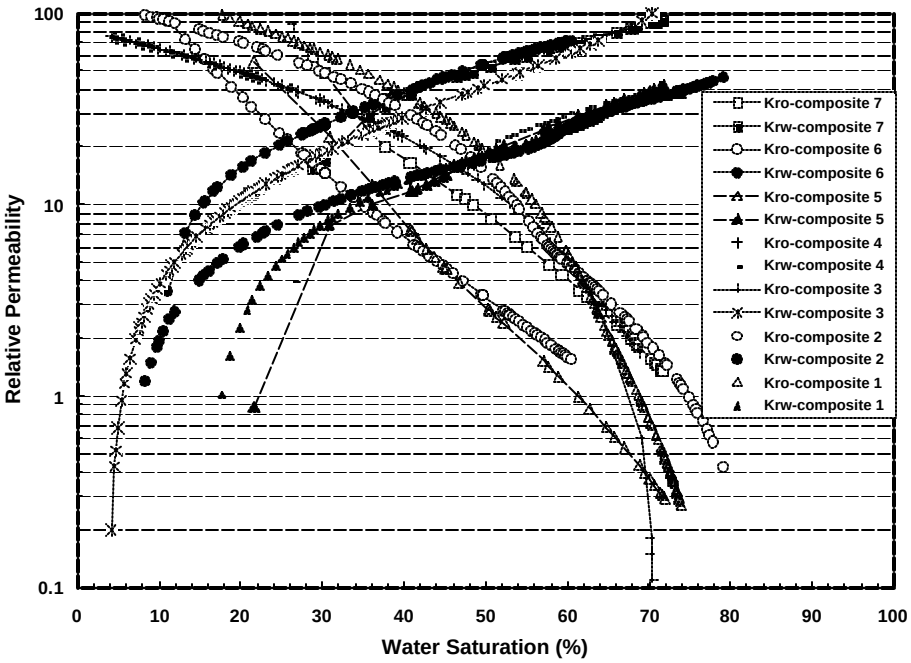

Figure 2: Unsteady-State Oil/Water Relative Permeability Curves for Arab-D Reservoir, Abu Safah Field.

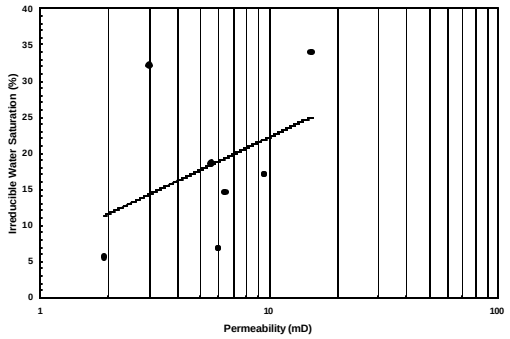

Figure 3: Irreducible Water Saturation vs. Stressed Permeability for Shu'aiba Reservoir, Shaybah Field.

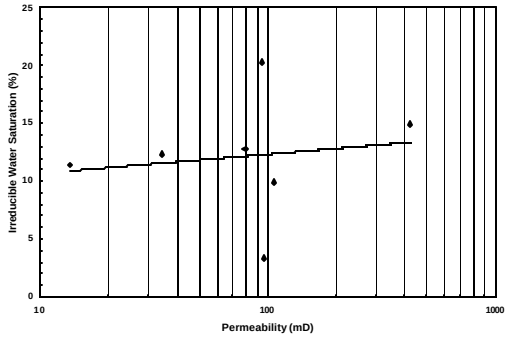

Figure 4: Irreducible Water Saturation vs. Stressed Permeability for Arab-D Reservoir, Abu Safah Field.

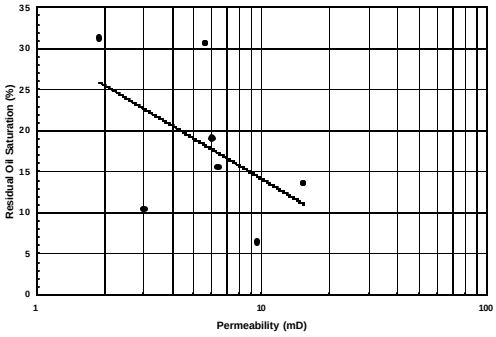

Figure 5: Residual Oil Saturation vs. Stressed Permeability for Shu'aiba Reservoir, Shaybah Field

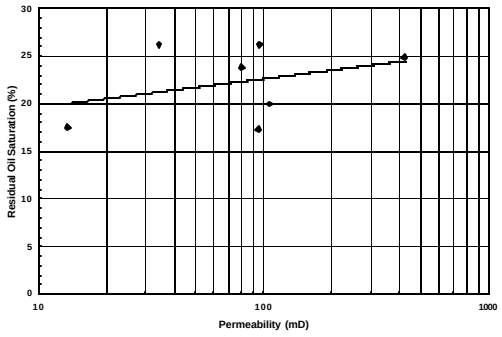

Figure 6: Residual Oil Saturation vs. Stressed Permeability for Arab-D Reservoir, Abu Safah Field

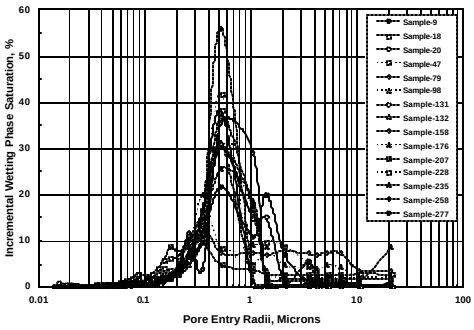

Figure 7: Pore Entry Radius vs. Incremental phase Saturation for Shu'aiba Reservoir, Shaybah Field

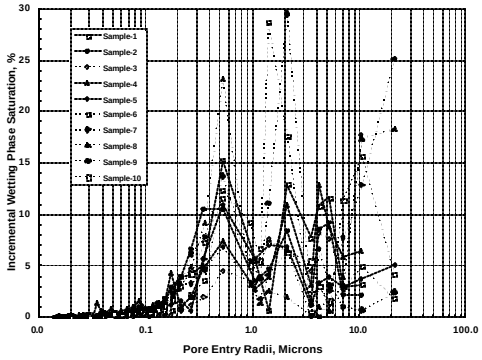

Figure 8: Pore Entry Radius vs. Incremental phase Saturation for Arab-D Reservoir, Abu Safah Field

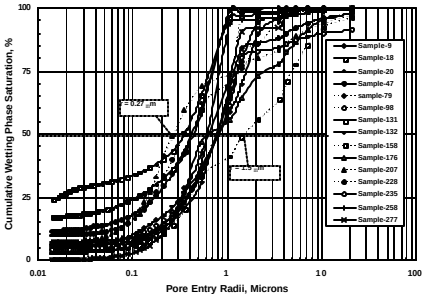

Figure 9: Pore Entry Radius vs Cumulative Wetting Phase Saturation for Shu'aiba Reservoir, Shaybah Field.

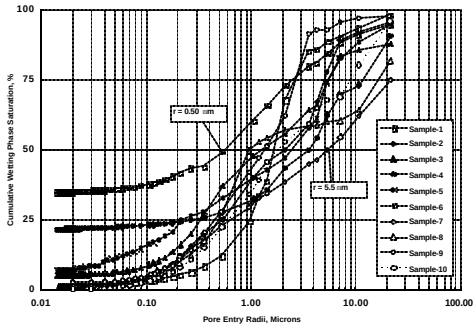

Figure 10: Pore Entry Radius vs Cumulative Wetting Phase Saturation for Arab-D Reservoir, Abu Safah Field.

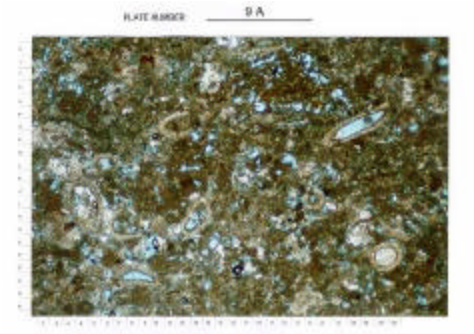

Figure 11: Non-dolomitic wackstone. Micro-porosity in inter-granular matrix. Dissolution of biogenic fragments leads to secondary porosity.

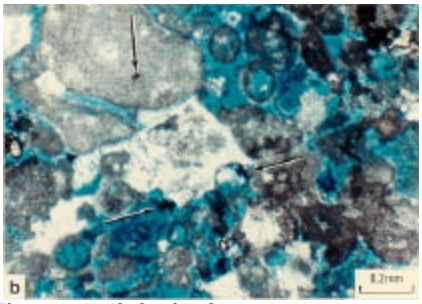

Figure 14: Skeletal-oolitic grainstone. Inter-particle and moldic macropores are abundant.

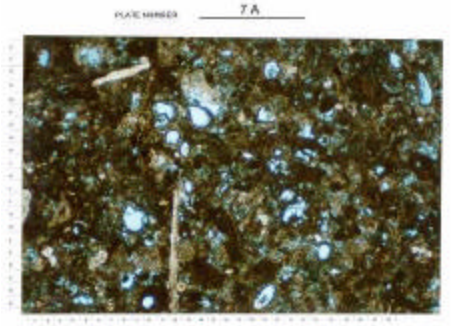

Figure 12: Packstone with deformable pelloids. Porosity developed through dissolution of biogenic fragments.

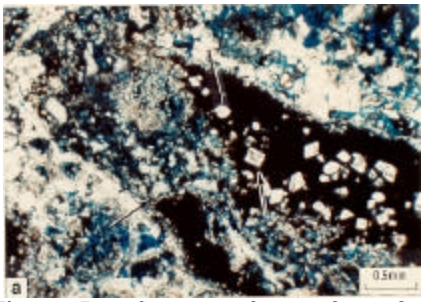

Figure 15: Dolomitic wackstone shows dissolution of inter-crystal mud to form inter-crystal pore space.

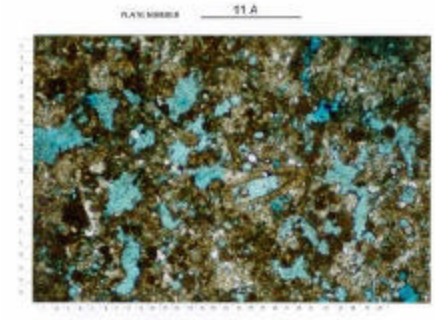

Figure 13: Packstone with considerable inter-granular porosity as a result of dissolution of the lime mud matrix. There are some relic pellets and biogenic debris.

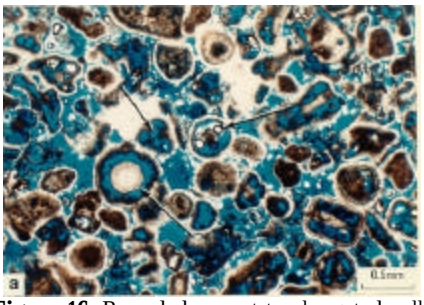

Figure 16: Rounded equant to elongated pelletoids with ooids texture. Moldic porosity and micropores matrix.